ROBUST CONTROL OF NET-ZERO OFFICES WITH INTEGRATED HYBRID SUPPLY SYSTEM AND ENERGY STORAGE

John Allison[a*]

[a] Energy Systems Research Unit, Dept. Mechanical & Aerospace Engineering, University of Strathclyde, 75 Montrose St., G1 1XJ, Glasgow, Scotland

*corresponding author: j.allison@strath.ac.uk

ABSTRACT

Commercial office buildings are a key target for energy reduction measures. One method of reducing commercial buildings' energy consumption is to make them more autonomous – creating more of their own energy, disposing of their own waste, collecting their own water; ultimately being as sustainable as possible (i.e. self-sustaining).

A move towards these energy autonomous systems could be accomplished by the use of renewable and co-generation energy sources. However, there are a multitude of these energy sources available, such as combined heat and power (CHP), thermal energy storage and electrical energy storage plants, heat pumps, photovoltaics, etc. Making these systems work together presents a control challenge for their efficient use, especially since they can have a simultaneous effect on both the thermal and electrical energy networks.

This paper describes a robust multi-input multi-output (MIMO) controller applicable to any configuration of the aforementioned systems, with the control goal of minimising the electrical grid utilisation of an office building while maintaining the thermal comfort of the occupants.

The controller employs the inverse dynamics of the building, mechanical/servicing systems, and energy storage with a robust control methodology. This inverse dynamics provides the controller with knowledge of the complex cause and effect relationships between the system, the controlled inputs, and the external disturbances, while an outer-loop control ensures robust, stable control in the presence of process uncertainty and unknown disturbances.

Results indicate that the control strategy is effective in minimising the electrical grid use and maximising the utilisation of the available renewable energy – towards net-zero office buildings – and shows the potential for deployment in future energy-autonomous office buildings.

Keywords: robust control, net-zero offices, energy storage, combined heat & power

INTRODUCTION

Commercial office buildings are a key target for energy reduction measures. One method of reducing commercial buildings' energy consumption is to make them more autonomous – creating more of their own energy, disposing of their own waste, collecting their own water; ultimately being as sustainable as possible (i.e. self-sustaining).

A move towards these energy autonomous systems could be accomplished by the use of renewable and co-generation energy sources. Combined heat and power (CHP) systems are a promising technology for these future energy autonomous offices as heat and power are simultaneously required during the operating hours of typical office buildings. Furthermore, due to the high thermal efficiencies and the production of immediately usable electricity, Stirling engine based CHPs are ideal for isolated or off-grid application [1]. However, the efficient use of CHP systems in off-grid applications presents a control challenge due to this simultaneous production of thermal and electrical energy – especially with no electrical buffer typically provided by the electrical grid to account for the intermittent nature of photovoltaics (PV), or when the CHP is unable to fulfil the demand.

Many of the current approaches to the control of these hybrid energy supply systems involves model predictive control [2, 3], and/or optimisation methods [4, 5]. These are very useful tools for determining the feasibility of a proposed energy supply system, or the optimal operational strategy provided the assumptions on the performance of the systems are in line with the those predicted by the models. However, the issue with these approaches is that they not only rely on models to predict the optimum operation regime, but rarely is attention given to the control strategy used *in operation* i.e. it is assumed that a thermally-led CHP is capable of providing the thermal load when it is required, and similarly for electrically-led systems.

These energy systems – and the external environment in which they operate – cannot be mod-

elled precisely, may change in an unpredictable manner, and may be subject to significant disturbances. The design of building energy management systems in the presence of significant uncertainty requires the development of a robust control system. Recent advances in robust control design methodologies can address stability robustness and performance robustness in the presence of uncertainty in the models.

The zone and plant models will always be an inaccurate representation of the actual system because of

- parameter changes
- unmodelled dynamics
- unmodelled time delays
- changes in equilibrium point (operating point)
- sensor noise
- unpredicted disturbance inputs.

The goal of robust systems design is to retain assurance of system performance in spite of model inaccuracies and changes. A system is robust when the system has acceptable changes in performance due to model changes or inaccuracies.

This disturbance attenuation is especially important in off-grid applications when considering the impact of an undersized or oversized system. For example, there may be occasions when the availability of the PV system energy exceeds both the power demand and the available storage capacity.

This paper describes a robust multi-input multi-output (MIMO) controller with a methodology that is applicable to any configuration of cogeneration and renewable energy systems, with the control goal of minimising the electrical grid utilisation of an office building while maintaining the thermal comfort of the occupants.

CONTROL THEORY

A robust control method of control allows the models to be imprecise, where the imprecision in this system stems from two major areas:

System uncertainty: It is not possible to know precisely the system parameters (e.g. the exact heat capacity of the building structure, or the heat transfer coefficients, or the vast array of disturbances to the system)

Simplified dynamics: The models used in this study are *purposefully* a simplified representation of the overall system (e.g. using a reduced model of the building structure, modelling the radiation heat transfer as linear, neglecting the modelling of the high frequency dynamical modes, such as internal mechanisms of the CHP plant or thermal store etc.)

In control literature, these two areas of imprecision are known as **structured** uncertainties (related to the parametric uncertainties) and **unstructured** uncertainties (the unmodelled or reduced-order dynamics) [6].

Robust controllers are comprised of two parts:

1. The inner model reduction component – commonly a feedback linearisation or inverse control law, and
2. An outer component used to account for the structured uncertainties

The following section details these two components of the controller that can be used for the robust control of hybrid energy supply systems in office buildings.

Nonlinear inversion control law

The differential equations that govern the dynamics of the office zone and its energy systems can be written in state-space form as the class of nonlinear MIMO control/input-affine systems described by

$$\begin{aligned} \dot{\boldsymbol{x}}(t) &= \boldsymbol{f}(\boldsymbol{x}(t)) + \boldsymbol{G}(\boldsymbol{x}(t))\boldsymbol{u}(t)\,, \\ \boldsymbol{y}(t) &= \boldsymbol{h}(\boldsymbol{x}(t))\,, \end{aligned} \tag{1}$$

where $\boldsymbol{x}(t) \in \mathbb{R}^n$ is the state vector, $\boldsymbol{y}(t) \in \mathbb{R}^m$ are the measured outputs, $\boldsymbol{u}(t) \subset U \in \mathbb{R}^m$, are the controlled inputs, $\boldsymbol{f} : \mathbb{R}^n \to \mathbb{R}^n$ and $\boldsymbol{h} : \mathbb{R}^n \to \mathbb{R}^m$ are smooth vector fields, and $\boldsymbol{G} : \mathbb{R}^n \to \mathbb{R}^n \times \mathbb{R}^m$ is a matrix whose columns $\boldsymbol{g}_j : \mathbb{R}^n \to \mathbb{R}^n$, $j = 1, \dots, m$ are smooth vector fields. Also, for notational compactness from now on the time-dependence is implied so that $\boldsymbol{x} \coloneqq \boldsymbol{x}(t)$, $\boldsymbol{u} \coloneqq \boldsymbol{u}(t)$, $\boldsymbol{y} \coloneqq \boldsymbol{y}(t)$.

The control objective is to make any output y_i (such as internal air temperature, or electrical grid power use) track a desired trajectory while keeping the system stable. The difficulty with this is that any output is only indirectly related to a controlled input, through the state variables and the nonlinear state equations. For example, a direct convective air heater will have a more deliberate effect on the air temperature that a hydronic radiator. The inability to quickly see a change in the output based upon a change in the controlled input often results in poor control and inefficient utilisation of the energy systems. In buildings a common result of this is over-heating/cooling.

A measure of this 'indirectness' is the relative order/degree of the output. From the mathematical representation of the system (1), it is possible to calculate the relative degree of each output in relation to the controlled input. This is determined by continually differentiating the output of the system

until the control appears:

$$\begin{aligned}\dot{y}_i &= \frac{\mathrm{d}h_i}{\mathrm{d}t} = \frac{\partial h_i}{\partial \boldsymbol{x}}\frac{\mathrm{d}\boldsymbol{x}}{\mathrm{d}t} = \mathcal{L}_{\boldsymbol{f}} h_i \\ \ddot{y}_i &= \frac{\partial \mathcal{L}_{\boldsymbol{f}} h_i}{\partial \boldsymbol{x}}\frac{\mathrm{d}\boldsymbol{x}}{\mathrm{d}t} = \mathcal{L}_{\boldsymbol{f}}^2 h_i \\ &\vdots \\ y_i^{(k)} &= \mathcal{L}_{\boldsymbol{f}}^k h_i\,, \quad \text{for } k < \rho_i \\ y_i^{(\rho_i)} &= \mathcal{L}_{\boldsymbol{f}}^{\rho_i} h_i + \sum_{j=1}^{m} \mathcal{L}_{\boldsymbol{g}_i}\mathcal{L}_{\boldsymbol{f}}^{\rho_i - 1} h_i u_j \end{aligned} \tag{2}$$

where $\mathcal{L}$ denotes the Lie derivative, and for at least one j, $\mathcal{L}_{\boldsymbol{g}_i}\mathcal{L}_{\boldsymbol{f}}^{\rho_i-1}h_i \neq 0$, and ρ_i denotes the relative degree of output y_i i.e. the relative degree corresponds to the lowest order derivative of the output that depends explicitly on an input.

The same method (2) can be applied to each output of the system (1) and written together in a single compact vector-matrix equation as

$$\underbrace{\begin{bmatrix} y_1^{(\rho_1)} \\ y_2^{(\rho_2)} \\ \vdots \\ y_m^{(\rho_m)} \end{bmatrix}}_{\hat{\boldsymbol{y}}} = \underbrace{\begin{bmatrix} \mathcal{L}_{\boldsymbol{f}}^{\rho_1} h_1 \\ \mathcal{L}_{\boldsymbol{f}}^{\rho_2} h_2 \\ \vdots \\ \mathcal{L}_{\boldsymbol{f}}^{\rho_m} h_m \end{bmatrix}}_{\boldsymbol{P}(\boldsymbol{x})} + \underbrace{\begin{bmatrix} \mathcal{L}_{\boldsymbol{g}_1}\mathcal{L}_{\boldsymbol{f}}^{\rho_1-1}h_1 & \dots & \mathcal{L}_{\boldsymbol{g}_m}\mathcal{L}_{\boldsymbol{f}}^{\rho_1-1}h_1 \\ \mathcal{L}_{\boldsymbol{g}_2}\mathcal{L}_{\boldsymbol{f}}^{\rho_2-1}h_2 & \dots & \mathcal{L}_{\boldsymbol{g}_m}\mathcal{L}_{\boldsymbol{f}}^{\rho_2-1}h_2 \\ \vdots & \dots & \vdots \\ \mathcal{L}_{\boldsymbol{g}_m}\mathcal{L}_{\boldsymbol{f}}^{\rho_m-1}h_m & \dots & \mathcal{L}_{\boldsymbol{g}_m}\mathcal{L}_{\boldsymbol{f}}^{\rho_m-1}h_m \end{bmatrix}}_{\boldsymbol{Q}(\boldsymbol{x})} \boldsymbol{u}$$

or

$$\hat{\boldsymbol{y}} = \boldsymbol{P}(\boldsymbol{x}) + \boldsymbol{Q}(\boldsymbol{x})\boldsymbol{u}\,. \tag{3}$$

If the matrix $\boldsymbol{Q}(\boldsymbol{x})$ in (3) is invertible, then utilising feedback control of the form

$$\boldsymbol{u} = (\boldsymbol{Q}(\boldsymbol{x}))^{-1}(-\boldsymbol{P}(\boldsymbol{x}) + \boldsymbol{v})\,, \tag{4}$$

results in the simple linear system

$$\begin{bmatrix} y_1^{(\rho_1)} \\ y_2^{(\rho_2)} \\ \vdots \\ y_m^{(\rho_m)} \end{bmatrix} = \begin{bmatrix} v_1 \\ v_2 \\ \vdots \\ v_m \end{bmatrix} \tag{5a}$$

$$\hat{\boldsymbol{y}} = \boldsymbol{v} \tag{5b}$$

where each v_i is an outer-loop control law to be defined in order to achieve the required performance tracking on y_i. It can be seen that utilising (4) has resulted in an input-output relation that is linearised *and* decoupled, such that each output y_i is a linear function of a single input v_i. For this reason (4) is called a **decoupling control law**, and the invertible matrix $\boldsymbol{Q}(\boldsymbol{x})$ is called the **decoupling matrix** of the system (1) [6].

Robust outer-loop control

The decoupling control law alone suffers the same drawbacks as model predictive control – in order to assure that the system has been decoupled and each v_i can be selected independently – relies on an accurate model of the system. However, is it possible to introduce a robust outer-loop control to account for the uncertainty in the model, and disturbances. The typical choice for the outer-loop controller is designed so that the output y_i asymptotically tracks the demand trajectory $y_{\mathrm{d},i}$. For example, in building and energy systems control, demand trajectories are typically the air temperature set-points. For this work, an outer-loop controller has been utilised that is a combination of local asymptotic stabilisation (via pole placement) and integral action. This type of control, known as pseudo-derivative-feedback (PDF) control, was pioneered by Phelan [7] as an alternative to the traditional proportional-integral (PI) controller that is used in most of cases in the industry. This control has been proven to perform better than PI when the relative order of the output is less than two ($\rho_i \leq 2$), but is also applicable to systems with a order of greater than two – to which PI control is not suitable since the order is higher than the degrees of freedom provided by the controller. The superior performance is gained by not introducing zeros into the system (which PI control does), allowing for a faster transient response with less overshoot.

The PDF control is given by

$$v_i = r_i - \sum_{q=1}^{\rho_i} K_{\mathrm{d}q} y_i^{(q-1)}\,, \quad i = 1, \dots, m \tag{6}$$

where $\dot{r}_i = K_{\mathrm{i},i} e_i$ and $\boldsymbol{k}_i = (K_{\mathrm{I},i}, K_{\mathrm{d}1}, \dots, K_{\mathrm{d}\rho_i})$ are the controller gains.

In order to demonstrate the performance of this control, and the selection of the controller gains $\boldsymbol{k}_i$, substituting (6) into a single output of (5a), and taking the Laplace transform results in the following transfer function between the demand trajectory and the output:

$$G_i(s) = \frac{Y_i(s)}{Y_{\mathrm{d},i}(s)} = \frac{K_{\mathrm{I},i}}{s^{\rho_i+1} + \sum_{j=1}^{\rho} K_{\mathrm{d}j} s^j + K_{\mathrm{I},i}} \tag{7}$$

Note that the introduction of the integral action has increased the order of the system by one. Now the controller gains $\boldsymbol{k}_i$ are selected so that the denominator of (7) forms a Hurwitz polynomial, which ensures all the poles are in the left-half plane – resulting in a stable system. System performance can then be tuned via any pole-placement technique to get the required tracking performance.

This combination of a inversion based control law and PDF control was originally developed in the aerospace and robotics industry [8], and more recently applied to the controllability of buildings [9]. However, the theory was only developed for application to the control of 'fast' system modes i.e. was only originally applicable to MIMO systems where the outputs were of relative order of one or less. Therefore, the theory presented in this

section is a generalisation of this work not only to the nonlinear inversion, but also extending the PDF control to higher-order systems.

System/actuator limits

The performance of all real systems is limited by the capabilities of the actuators that are responsible for the transfer of energy from the control system to the process being controlled. The actuating control value that supplies fuel to the CHP engine has a maximum and minimum fuel supply, as well as restricted rate at which the fuel can be delivered. Electrical energy storage also has low-level electronics that restricts the maximum permissible current that can be transferred to the device to avoid overheating and to protect their inner circuitry. Depending on the type of thermal energy store, these can have mechanical/hydraulic actuators that have physical limits on the magnitude or flow rate of water entering/exiting from the tank. Many of these discontinuous limits are designed to ensure safe performance of the energy system, and so the 'high-level' controller should be respectful of these system limitations to ensure optimal and safe control.

There are many cases when a system may reach the limits of the actuator; this can be when there is a large change in set-point such that the system must drive as hard as possible to reach its target. There is also the case where a large disturbance may cause the actuator to saturate. A well-designed controller should be capable of handling *exceptional* disturbances, i.e. disturbances of intensity higher than the predicted bounds which are used when tuning the control parameters. If integral control is used in such cases, the integral term in the control action may become unreasonably large, so that once the disturbance stops, the system goes through large amplitude oscillations in order to return to the desired trajectory.

Fortunately, it is possible to compensate for these control limitations.

If the system is well designed, the final control elements will be capable of supplying the energy required by the controlled system to insure that the controlled variable follows the reference set-point within the performance specifications over the specified linear range of operation. Under such circumstances, the only way a reasonably well tuned system can get into trouble is for it to be driven into the saturation region.

A common and potentially obvious way to avoid integrator wind-up is to avoid saturating the actuator in the first place. This can be achieved by appropriately sizing the energy supply systems and their actuators so that it is always able to supply any potential demand for energy. However, this will often not be practical or efficient, since maximum/peak demand may only occur for a limited time during the lifetime of the system if they were to be sized this way. Also most energy supply systems are at their most efficient when running at full load, so operating at (but not beyond) the actuator limits can actually be the most energy efficient control option.

Another option is to 'de-tune' the control system, so that its response to large errors is slower, which will in turn smooth the changes in the control signal such that it avoids entering the saturation region. Obviously this will lead to a downturn in controller performance that will almost always be unacceptable or fall far from the performance specifications. Again, this is especially true for the control of energy supply systems since they must react quickly to the electrical and thermal demands of the building.

The final, and most affective way to cope with integrator wind-up is to design a variable structure controller so that when the controller output has reached either limit, any future control action must either keep u_i constant or reduce it so that it will continue its normal linear mode of operation [8]. Mathematically this can be expressed as:

$$u\dot{u} \leq 0 \qquad \text{when } u \geq v_{\max} \vee u \leq v_{\min}\,. \tag{8}$$

If (8) can be ensured, then the controller output u will always tend to decrease away from the saturation limit.

To implement this new switching surface with a PDF controller, first define the following nonlinear piecewise 'dead zone' function, where for an given input u, the output $\tilde{u}$ is given by

$$\tilde{u} = \begin{cases} 0 & \text{if } v_{\min} \leq u \leq v_{\max} \\ u - v_{\max} & \text{if } u > v_{\max} \\ u - v_{\min} & \text{if } u < v_{\min} \end{cases} \tag{9}$$

Then from (9), when $\tilde{u} \neq 0$ then the system has been overdriven as the controller output, u, is out with the physical limits $(v_{\min}, v_{\max})$. This can be represented as the logical function:

$$\texttt{isSaturated} \coloneqq \tilde{u} \neq 0\,. \tag{10}$$

The other aspect of the integrator clamping logic, is determined by the direction of the system – if the error signal would cause the system to move further into the saturation region then the integrator should be clamped. This is determined easily by realising that when the sign of the error, $\mathrm{sgn}(e)$, is the same as that of $\tilde{u}$ then the system will be pushed further into the saturation region. This is easily represented by the following logical function:

$$\texttt{isIncreasing} \coloneqq e \cdot \tilde{u} > 0\,. \tag{11}$$

Then the new integrator clamping logic can be implemented as

$$\dot{r} = \begin{cases} 0 & \text{if } \texttt{isSaturated} \wedge \texttt{isIncreasing} \\ K_{\mathrm{i}} e & \text{otherwise} \end{cases} \tag{12}$$

The synthesis of the nonlinear variable structure inversion control law, the outer-loop PDF control, and final control elements is given in the block diagram schematic of fig. 1.

Special theory: Linear systems

Although all real systems are nonlinear, there are systems which either predominately perform as linear systems, where the dynamics are given as a set of first-order ordinary differential equations (ODEs), or the system operates around a local equilibrium point. This is also applicable to a subset of building control problems such as well insulated buildings and energy systems which have a limited range of operation. For these cases, small signal analysis applies and the behaviour of the system can be well approximated as a linear system. In any case, the nonlinear system (1) can be linearised via the Jacobian linearisation approach. Define

$$\boldsymbol{A} \coloneqq \left[\frac{\partial \boldsymbol{f}}{\partial \boldsymbol{x}}\right]_{(\boldsymbol{x}_{\mathrm{e}}, \boldsymbol{u}_{\mathrm{e}})} \qquad \boldsymbol{B} \coloneqq \left[\frac{\partial \boldsymbol{f}}{\partial \boldsymbol{u}}\right]_{(\boldsymbol{x}_{\mathrm{e}}, \boldsymbol{u}_{\mathrm{e}})}$$

$$\boldsymbol{C} \coloneqq \left[\frac{\partial \boldsymbol{h}}{\partial \boldsymbol{x}}\right]_{(\boldsymbol{x}_{\mathrm{e}}, \boldsymbol{u}_{\mathrm{e}})} \qquad \boldsymbol{D} \coloneqq \left[\frac{\partial \boldsymbol{h}}{\partial \boldsymbol{u}}\right]_{(\boldsymbol{x}_{\mathrm{e}}, \boldsymbol{u}_{\mathrm{e}})}$$

Then the system becomes

$$\begin{aligned} \dot{\boldsymbol{x}} &= \boldsymbol{A}\boldsymbol{x} + \boldsymbol{B}\boldsymbol{u}\,, \\ \boldsymbol{y} &= \boldsymbol{C}\boldsymbol{x} + \boldsymbol{D}\boldsymbol{u}\,. \end{aligned} \tag{13}$$

Applying the method (2) to the linear system (13) is straightforward and results in $\mathcal{L}_{\boldsymbol{f}}^{k} h_i = \boldsymbol{c}_i \boldsymbol{A}^k \boldsymbol{x}$ and $\mathcal{L}_{\boldsymbol{g}_k} \mathcal{L}_{\boldsymbol{f}}^{k} h_i = \boldsymbol{c}_i \boldsymbol{A}^k \boldsymbol{B}$. Then, the subsystem of relative order ρ_i that directly relates an input to the output y_i is given by

$$y_i^{(\rho_i)} = \boldsymbol{c}_i \boldsymbol{A}^{\rho_i} \boldsymbol{x} + \boldsymbol{c}_i \boldsymbol{A}^{\rho_i - 1} \boldsymbol{B}\boldsymbol{u}\,. \tag{14}$$

Utilising the same feedback control as (4) results in the decoupling control law for linear systems where the elements $\boldsymbol{P}(\boldsymbol{x}) = \boldsymbol{P}\boldsymbol{x}$ and $\boldsymbol{Q}$ are defined as

$$\boldsymbol{P}\boldsymbol{x} = \begin{bmatrix} \boldsymbol{c}_1 \boldsymbol{A}^{\rho_1} \\ \boldsymbol{c}_2 \boldsymbol{A}^{\rho_2} \\ \vdots \\ \boldsymbol{c}_m \boldsymbol{A}^{\rho_m} \end{bmatrix} \boldsymbol{x} \qquad \boldsymbol{Q} = \begin{bmatrix} \boldsymbol{c}_1 \boldsymbol{A}^{\rho_1 - 1} \boldsymbol{B} \\ \boldsymbol{c}_2 \boldsymbol{A}^{\rho_2 - 1} \boldsymbol{B} \\ \vdots \\ \boldsymbol{c}_m \boldsymbol{A}^{\rho_m - 1} \boldsymbol{B} \end{bmatrix} \tag{15}$$

Note that for linear systems, the decoupling matrix $\boldsymbol{Q}$ is static and is not a function of the state. Therefore, provided reasonable estimates of the system parameters, the system can be decoupled without state measurement or estimation.

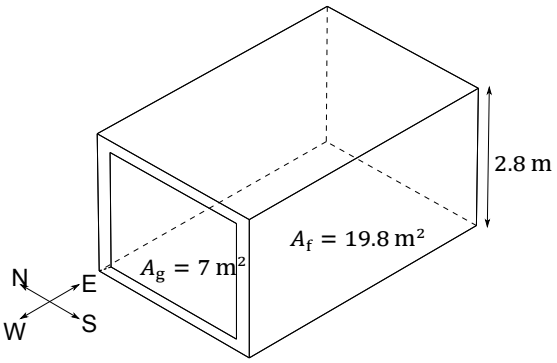

Figure 2: Wire frame drawing of office zone

Inverse dynamics

It is possible by utilising (4), and assuming that all disturbance inputs are known, to find out what initial conditions and control input $\boldsymbol{u}$ should be in order for the system output to track a reference output perfectly. This can be useful for several purposes; namely ideal control in building simulation. With the controller implemented in a building simulation, it is possible to determine the feasibility of a proposed combination of energy systems, and then the related sizing of the aforementioned systems. Then, the real-world control strategy implemented would incorporate the robust outer-loop control strategy in order to account for unmeasured disturbances, parameter uncertainty, and unmodelled dynamics.

This could be incorporated into the building design stage, whereby the appropriate mix and size of energy systems for a proposed building can be determined in building simulation via inverse dynamics, and then the real-world controller implemented based upon these models and the robust control strategy presented herein.

What follows is a case study applied to a small office zone that has a complex hybrid energy supply system.

CASE STUDY

The zone modelled is a small office located in Trappes, France, for which the climatic data (external air temperature and solar radiation) is available. Figure 2 shows the wire-frame drawing of a single office zone, with major dimensions indicated. The overall office controlled consists of four of these zones in parallel, joined along their length so that all windows are facing west. The thermal demands of the zone are served by a hydronic radiator system supplied by a Stirling-engine based CHP system. The electrical demands are fulfilled by the electrical generation of the CHP, PV, and electrical energy storage. The chosen control objective is to make the measured air temperature track a desired trajectory while minimising the electrical grid utilisation. The dif-

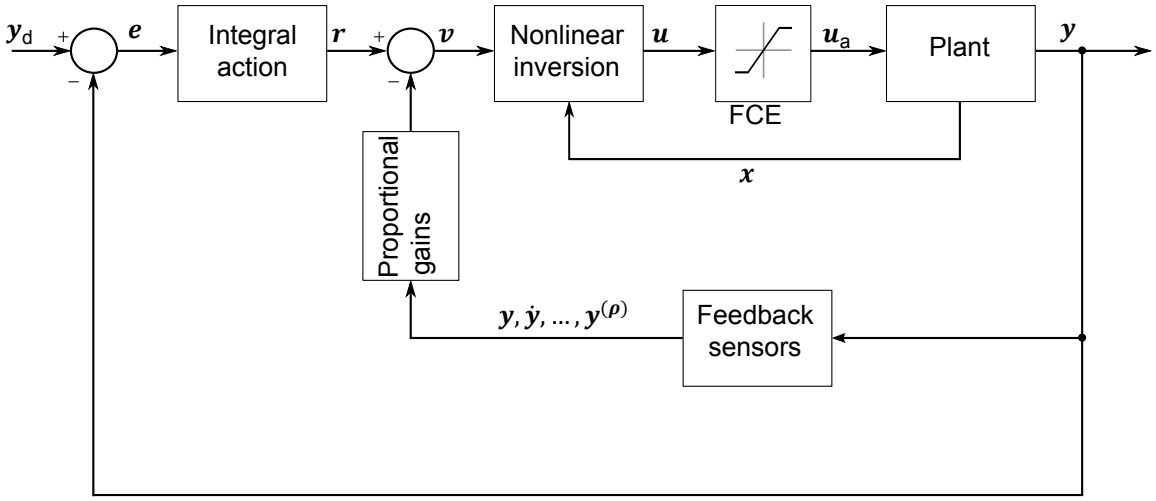

Figure 1: Schematic of control theory

ficulty is that the air temperature is only indirectly related to the input fuel flow rate – which must first influence the engine, cooling water, and radiator temperatures before changes to the internal air temperature will be seen. The number of 'elements' or states downstream of the control input are related to the relative order/degree of that output discussed earlier.

Therefore, it is not easy to see how the input can be designed to control the tracking behaviour of the output. This configuration of systems is well suited to the application of the control theory presented in the previous section.

System specifications

The CHP specifications are based upon a WhisperGEN CHP engine, with empirical data taken from [10]. The engine has an external pump, and a permissible water flow rate of $3\,\mathrm{l\,min^{-1}}$ to $8\,\mathrm{l\,min^{-1}}$. It is assumed that the lower heating value of the fuel supply to the engine is $LHV_{\mathrm{fuel}} = 35.16\,\mathrm{MJ\,kg^{-1}}$. This particular engine has a small electrical capacity of $750\,\mathrm{W}$ (nominal) – equivalent to $575\,\mathrm{W}$ once the parasitic electrical consumption of the CHP is subtracted – and large thermal output $6.5\,\mathrm{kW}$ (nominal). The typical application is residential micro CHP, but is shown here to be applicable to an array of small office zones. Where it may be possible in the future to use multiple micro CHP units throughout a larger building to serve specific levels or zones within the larger whole. These engines are typically controlled by heat demand (heat-led) rather than electrical demand. The control developed here is 'led-agnostic', as the CHP is operated based upon the prevailing demands of both the thermal and electrical networks due to the decoupling control law.

The unit also has several low-level controls: The unit will shutdown if the cooling water temperature at the outlet of the system exceeds $85\,^{\circ}\mathrm{C}$. The cool-down period of the unit was $25\,\mathrm{min}$, but is assumed that the cool-down period is *optional*, that is if the unit receives demand while in cool-down mode it will switch to warm-up before completing the entire cool-down period.

For the purpose of control demonstration, it is assumed that the unit can also modulate down to as low as $3\,\mathrm{kW}$, while still generating electricity. Furthermore, a fixed efficiency and heat-to-power ratio is also assumed.

The results given here are calculated using two reference inputs. The first is the operative temperature (in this case the air temperature of the zone). This heating set-point is $20\,^{\circ}\mathrm{C}$ between 08:00 and 18:00 on weekdays, with a night time and weekend setback temperature of $12\,^{\circ}\mathrm{C}$. The cooling has been disabled for these simulations in order to draw closer comparisons between different configurations that may not lend themselves to incorporating cooling, as such, a cooling device has not been included in this set of results. The second is the electrical grid power set-point, which is set to zero. This means that the controller will strive to neither import or export from or to the national grid, thereby minimising the use of the grid.

The internal gains are defined per floor area at $20\,\mathrm{W\,m^{-2}}$ and are defined as $50\,\%$ convective to the internal air of the zone and $50\,\%$ radiative to the walls and floor. The electrical loads are comprised of the internal gains, at $20\,\mathrm{W\,m^{-2}}$, which equates to a standing load of $396\,\mathrm{W}$ for each cell between 08:00 and 18:00 during weekdays.

The energy production from photovoltaics is calculated using PVWatts [11]. The PV system characteristics consist of a $650\,\mathrm{W}$ solar array, south facing with a fixed tilt of $48.73°$ (which is equal to the latitude of the climate data).

Electrical grid measurement

The theoretical electrical grid use is based upon an energy balance with all demand and supply elements given by:

$$y_2 = P_{\text{grid}} = P_{\text{load}} - P_{\text{bat}} - P_{\text{pv}} - P_{\text{chp}} \quad (16)$$

It can be seen from (16) that the availability of PV is considered a disturbance. In this way, priority is given to utilising as much of the PV-generated electricity as possible, while the CHP can compensate for the remaining demand.

However, note that in (16) the control is immediately affecting the output of the system i.e. the electrical grid output has a relative degree of zero, that is, the manipulated fuel flow rate and battery (dis/)charge instruction has an immediate and direct effect on the interaction with the electrical grid.

Although the theory can be amended to account for such systems by making the control input be its rate-of-change i.e. $\dot{u}_2$ would become the new control input. However, a more robust approach is to use the output-redefinition method, whose principle is to redefine the output function so that the original control theory can be utilised. Provided that the new output function is defined in such a way that it is essentially the same as the original output function in the frequency range of interest, exact tracking of the new output function then also implies good tracking of the original output y_i. i.e. the electrical grid regulation will still be achieved since the outer-loop compensator will drive the actual output to zero. This method is preferable to the first, since the first method can introduce large chattering in the control input if there is any measurement noise in the electrical grid output.

The output-redefinition method is achieved by introducing an additional state for the electrical grid power, given by

$$\dot{x}_{\text{grid}} = 1/\tau_{\text{grid}}(P_{\text{grid}} - x_{\text{grid}}) \quad (17)$$

This increases the relative order of the electrical grid output by one, so that (4) can be implemented directly. The time constant τ_{grid} dictates how quickly the control model will estimate the actual grid use.

Plant models

There are a number of Stirling-engine based dynamicCHP models in the literature [12–14] but the Annex 42 model [15] was selected for this work as it was the simplest model that was still independently empirically validated [16]. The engine model consists of three control volumes (subsystems): (1) Energy conversion, (2) engine, (3) cooling water. These subsystems are described briefly here to facilitate understanding and how the control operates. Original validation has of the model was carried out in [17].

Energy conversion control volume:

$$P_{\text{chp}} = \eta_{\text{e}}\Phi_{\text{gross}} \quad (18)$$

$$\Phi_{\text{gen}} = \eta_{\text{q}}\Phi_{\text{gross}} \quad (19)$$

$$\Phi_{\text{gross}} = \dot{m}_{\text{fuel}}LHV_{\text{fuel}} \quad (20)$$

Engine control volume:

$$C_{\text{eng}}\dot{\Theta}_{\text{eng}} = \Phi_{\text{gen}} - \Phi_{\text{HX}} - \Phi_{\text{skin-loss}} \quad (21)$$

Cooling water control volume:

$$C_{\text{cw}}\dot{\Theta}_{\text{cw}} = [\dot{m}c_p]_{\text{cw}}(\Theta_{\text{rad,2}} - \Theta_{\text{cw}}) + \Phi_{\text{HX}} \quad (22)$$

where $\Phi_{\text{HX}} = H_{\text{HX}}(\Theta_{\text{eng}} - \Theta_{\text{cw}})$.

Radiator (2-node) model:

$$C_{\text{rad}}\dot{\Theta}_{\text{rad,1}} = [\dot{m}c_p]_{\text{cw}}(\Theta_{\text{cw}} - \Theta_{\text{rad,1}}) \quad (23)$$

$$C_{\text{rad}}\dot{\Theta}_{\text{rad,2}} = [\dot{m}c_p]_{\text{cw}}(\Theta_{\text{rad,1}} - \Theta_{\text{rad,2}}) - \Phi_{\text{rad}} \quad (24)$$

where

$$\Phi_{\text{rad}} = \frac{\Phi_0}{\Delta\Theta_0{}^{n_{\text{r}}}}\left[\frac{\Theta_{\text{rad,1}} - \Theta_{\text{rad,2}}}{\ln\left(\frac{\Theta_{\text{rad,1}} - \Theta_{\text{e}}}{\Theta_{\text{rad,2}} - \Theta_{\text{e}}}\right)}\right]^{n_{\text{r}}},$$

and $\Theta_{\text{e}} \approx \frac{\Theta_{\text{a}}+\Theta_{\text{s}}}{2}$.

Building model

The building model utilised in the work is a simplified dynamic building model with energy performance results validated [18] with European Standard EN 15265 [19]. Each enclosure component (e.g. wall, floor, ceiling) are assigned two thermodynamic temperature nodes according to the theory of [20], which can account for the fluctuations seen on either side of a construction in typical residential and office zones.

Air temperature node:

$$C_{\text{a}}\dot{\Theta}_{\text{a}} = \sum_{j=1}^{m} h_{\text{ci}}A_j(\Theta_{\text{s},j} - \Theta_{\text{a}}) + H_{\text{loss}}(\Theta_{\text{e}} - \Theta_{\text{a}}) + \Phi_{\text{rad}} + \Phi_{\text{load}} + \Phi_{\text{sol}} \quad (25)$$

Structural node:

$$C_{\text{s},j} = h_{\text{ci}}(\Theta_{\text{a}} - \Theta_{\text{s},j} + (1/R_{\text{cp},j})(\Theta_{\text{si}} - \Theta_{\text{s}}j) \quad (26)$$

The overall system to be controlled can be expressed in a general state-space form by combining the zone equations and plant models and selecting the state vector $\boldsymbol{x}$ as $\boldsymbol{x} = (\Theta_{\text{a}}, \Theta_{\text{s1}}, \dots, \Theta_{\text{s},m})$

and the control inputs $\boldsymbol{u} = (\dot{m}_{\text{fuel}}, P_{\text{bat}})$, the measured exogenous signals as $\boldsymbol{w} = (P_{\text{load}}, P_{\text{pv}})$, disturbances as $\boldsymbol{d} = (\Theta_{\text{e}}, \Phi_{\text{sol}})$ and system outputs $\boldsymbol{y} = (\Theta_{\text{a}}, P_{\text{grid}})$

The inversion control-law does not assume knowledge of any of the disturbance signals to the model, these are compensated for by the outer-loop control. Increased control performance could be attained by incorporating an estimate of the disturbances, such as the rate of heat loss to the outside environment.

While the theory can be applied to the nonlinear system directly, the computational effort to calculate the inverse is much greater. Furthermore, the nonlinear dynamics of the system are governed by the $\boldsymbol{f}(\boldsymbol{x})$ term, which is due to the radiator model. Since the fluctuations with the building are relatively small, the local linear system (13) will be sufficient for control model purposes. Furthermore, the modelling inaccuracies are addressed by the use of the outer-loop PDF control, which compensates for the matched disturbances and parameter inaccuracies.

Preliminary results

Figures 3 and 4 show the dynamic results from the model with robust control law for a cold, bright day. The sampling frequency of the controller was set to $0.5\ \text{Hz}$. Best performance and accurate simulation from the numerical solver is achieved when the update period of the controller is set four to five times faster than the slowest time constant in the system.

As can be seen in fig. 3, the control is able after a stable transient period to maintain the set-point temperature with no oscillation or 'ringing' around the set-point typically associated with thermally-led CHP switching on and off to fulfil the demand.

Figure 4 shows all of the elements of the electrical network working together to achieve zero electrical grid interaction. This demonstrates the strength of the robust control strategy as it is able to balance both the thermal and electrical networks without any reliance upon the electrical grid.

CONCLUSION

A robust nonlinear control strategy has been presented, with potential application to a vast array of hybrid energy supply systems that have coupled electrical and thermal demands – with the goal of minimising the interaction with the national grid – and move towards energy autonomous offices.

The control is a pragmatic solution that runs in real-time without knowledge of the external environment or future prediction of zone use or availability of energy sources. It is also respectful of un-

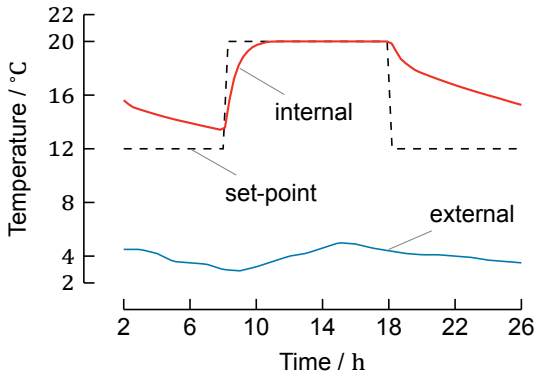

Figure 3: Dynamic response – temperature

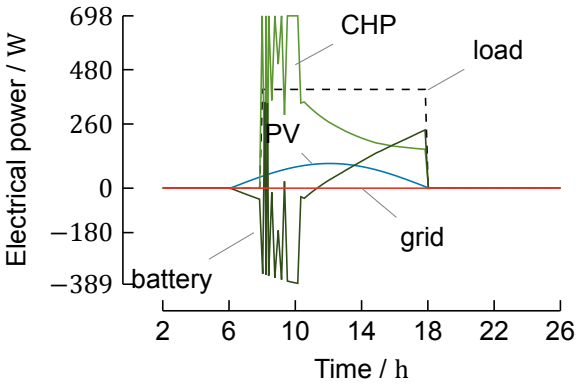

Figure 4: Dynamic response – Electrical power

dersized heating systems and actuating elements so that the system remains stable and achieves best possible performance in the face of parameter uncertainty and modelling inaccuracies.

Only preliminary results have been presented here, as the emphasis was placed on the underlying theory and its application to general energy systems. Future work will detail its application to larger and more in-depth case studies, with the ultimate goal of field trials with physical systems out with the simulation environment.

NOMENCLATURE

Φ_{gross}	gross heat input into the system (W)
$\dot{m}_{\text{fuel}}$	fuel flow rate ($\mathrm{kg\,s^{-1}}$)
LHV_{fuel}	lower heating value of fuel ($\mathrm{J\,kg^{-1}}$)
P_{net}	electrical output of CHP engine (W)
η_{e}	CHP electrical efficiency ($-$)
Φ_{gen}	rate of generation within CHP (W)
η_{q}	part load, thermal efficiency of the CHP engine ($-$)
C_i	thermal capacitance of state ($\mathrm{W\,K^{-1}}$)
Φ_{HX}	rate of heat transfer to the cooling water (W)
$\Phi_{\text{skin-loss}}$	rate of heat loss from the unit (W)
Θ_{eng}	bulk temperature of engine (°C)
Φ_0	Nominal radiator output (W)
$\Delta\Theta_0$	Nominal radiator inlet-outlet temperature (°C)
Θ_{e}	Environmental temperature

REFERENCES

[1] Carlos Ulloa, Pablo Eguía, José Luis Miguez, Jacobo Porteiro, José M. Pousada-Carballo, and Antón Cacabelos. Feasibility of using a Stirling engine-based micro-CHP to provide heat and electricity to a recreational sailing boat in different European ports. *Appl. Therm. Eng.*, 59(1-2):414–424, September 2013. ISSN 13594311. doi: 10.1016/j.applthermaleng.2013.06.015. URL http://www.sciencedirect.com/science/article/pii/S1359431113004298.

[2] Fabrizio Sossan, Henrik Bindner, Henrik Madsen, Dimitri Torregrossa, Lorenzo Reyes Chamorro, and Mario Paolone. A model predictive control strategy for the space heating of a smart building including cogeneration of a fuel cell-electrolyzer system. *Int. J. Electr. Power Energy Syst.*, 62:879–889, November 2014. ISSN 01420615. doi: 10.1016/j.ijepes.2014.05.040. URL http://www.sciencedirect.com/science/article/pii/S0142061514003111.

[3] Philipp Wolfrum, Martin Kautz, and Jochen Schäfer. Optimal control of combined heat and power units under varying thermal loads. *Control Eng. Pract.*, 30:105–111, September 2014. ISSN 09670661. doi: 10.1016/j.conengprac.2013.08.014. URL http://www.sciencedirect.com/science/article/pii/S0967066113001603.

[4] J. Kortela and S-L. Jämsä-Jounela. Modeling and model predictive control of the BioPower combined heat and power (CHP) plant. *Int. J. Electr. Power Energy Syst.*, 65: 453–462, February 2015. ISSN 01420615. doi: 10.1016/j.ijepes.2014.10.043. URL http://www.sciencedirect.com/science/article/pii/S0142061514006462.

[5] Mohammad H. Moradi, Mehdi Hajinazari, Shahriar Jamasb, and Mahmoud Paripour. An energy management system (EMS) strategy for combined heat and power (CHP) systems based on a hybrid optimization method employing fuzzy programming. *Energy*, 49:86–101, January 2013. ISSN 03605442. doi: 10.1016/j.energy.2012.10.005. URL http://www.sciencedirect.com/science/article/pii/S0360544212007670.

[6] Jean-Jacques E. Slotine and Weiping Li. *Applied Nonlinear Control*. Prentice Hall, New Jersey, 1991. ISBN 0-13-040890-5.

[7] Richard M Phelan. *Automatic control systems*. Cornell University Press, London, UK, 1977. ISBN 0-8014-1033-9.

[8] A Bradshaw and John Mark Counsell. Design of autopilots for high performance missiles. *Proc. Inst. Mech. Eng. Part I J. Syst. Control Eng.*, 206(2):75–84, May 1992. doi: 10.1243/pime_proc_1992_206_313_02. URL http://pii.sagepub.com/content/206/2/75.

[9] John Mark Counsell, Yousaf Ali Khalid, and Joseph Brindley. Controllability of buildings: A multi-input multi-output stability assessment method for buildings with slow acting heating systems. *Simul. Model. Pract. Theory*, 19(4):1185–1200, April 2011. doi: 10.1016/j.simpat.2010.08.006. URL http://www.sciencedirect.com/science/article/pii/S1569190X10001826.

[10] Ulli Arndt, Ian Beausoleil-Morrison, Mark Davis, William D'haeseleer, Viktor Dorer, Evgeuniy Entchev, Alex Ferguson, John Gusdorf, Nick Kelly, Marianne Manning, Leen Peeters, Maurizio Sasso, Daniel Schreiber, Sergio Sibilio, Kathleen Siemens, and Mike Swinton. Experimental Investigation of Residential Cogeneration Devices and Calibration of Annex 42 Models. Technical report, Annex 42 of the International Energy Agency Energy Conservation in Buildings and Community Systems Programme, 2007.

[11] National Renewable Energy Laboratory. PVWatts, 2012. URL http://rredc.nrel.gov/solar/calculators/PVWATTS/version1/.

[12] G. Conroy, A. Duffy, and L.M. Ayompe. Validated dynamic energy model for a Stirling engine μ-CHP unit using field trial data from a domestic dwelling. *Energy Build.*, 62:18–26, July 2013. ISSN 03787788. doi: 10.1016/j.enbuild.2013.01.022. URL http://www.sciencedirect.com/science/article/pii/S0378778813000534.

[13] Hoseong Lee, John Bush, Yunho Hwang, and Reinhard Radermacher. Modeling of micro-CHP (combined heat and power) unit and evaluation of system performance in building application in United States. *Energy*, 58:364–375, September 2013. ISSN 03605442. doi: 10.1016/j.energy.2013.05.015. URL http://www.sciencedirect.com/science/article/pii/S036054421300399X.

[14] J. Godefroy, R. Boukhanouf, and S. Riffat. Design, testing and mathematical modelling of a small-scale CHP and cooling system (small CHP-ejector trigeneration). *Appl. Therm. Eng.*, 27(1):68–77, January 2007. ISSN 13594311. doi: 10.1016/j.applthermaleng.2006.04.029. URL http://www.sciencedirect.com/science/article/pii/S135943110600175X.

[15] Ian Beausoleil-Morrison, Alex Ferguson, Brent Griffith, Nick Kelly, François Maréchal, and Andreas Weber. Specifications for Modelling Fuel Cell and Combustion-Based Residential Cogeneration Devices within Whole-Building Simulation Programs. Technical report, Annex 42 of the International Energy Agency Energy Conservation in Buildings and Community Systems Programme, 2007. URL www.cogen-sim.net.

[16] A. Rosato and S. Sibilio. Calibration and validation of a model for simulating thermal and electric performance of an internal combustion engine-based micro-cogeneration device. *Appl. Therm. Eng.*, 45-46:79–98, December 2012. ISSN 13594311. doi: 10.1016/j.applthermaleng.2012.04.020. URL http://www.sciencedirect.com/science/article/pii/S1359431112002633.

[17] Ian Beausoleil-Morrison and Alex Ferguson. Inter-model Comparative Testing and Empirical Validation of Annex 42 Models for Residential Cogeneration Devices. Technical report, Annex 42 of the International Energy Agency Energy Conservation in Buildings and Community Systems Programme, 2007.

[18] John Allison, Gavin Bruce Murphy, and John Mark Counsell. Control of micro-CHP and thermal energy storage for minimising electrical grid utilisation. *Int. J. Low-Carbon Technol.*, August 2014. doi: 10.1093/ijlct/ctu023. URL http://ijlct.oxfordjournals.org/content/early/2014/08/20/ijlct.ctu023.abstract.

[19] BS EN 15265:2007. *Energy performance of buildings. Calculation of energy needs for space heating and cooling using dynamic methods. General criteria and validation procedures*. British Standards Institution, London, UK, 1 edition, 2007. ISBN 978-0-580-55627-2. doi: 10.3403/30136887. URL https://bsol.bsigroup.com/Bibliographic/BibliographicInfoData/000000000030136887.

[20] Alfonso P. Ramallo-González, Matthew E. Eames, and David A. Coley. Lumped parameter models for building thermal modelling: An analytic approach to simplifying complex multi-layered constructions. *Energy Build.*, 60:174–184, May 2013. ISSN 03787788. doi: 10.1016/j.enbuild.2013.01.014. URL http://www.sciencedirect.com/science/article/pii/S0378778813000315.